

Cover letter

Reykjavik 3rd December 2020.

Dear Peter Landschützer,

I thank you for very constructive comments on how to respond on the alkalinity issue and improve the manuscript. We agree with you on the need to provide further results and I hope you find the additional evidence on alkalinity we present sufficient. It is basically in Table 2, in Figure 6 and in the Results and Discussion sections.

The main text and the supplement have been extensively revised. The responses to reviewers 1 and 2 have been edited slightly to show how we have reacted to their comments. We submit the revised responses.

We look forward to hearing from you.

Yours sincerely,

Jón Ólafsson.

1 **Enhancement of the North Atlantic CO<sub>2</sub> sink by Arctic Waters**

2 Jon Olafsson<sup>1</sup>, Solveig R. Olafsdottir<sup>2</sup>, Taro Takahashi<sup>3,5</sup>, Magnus Danielsen<sup>2</sup> and Thorarinn  
3 S. Arnarson<sup>4,5</sup>

4  
5 <sup>1</sup> Institute of Earth Sciences, Sturlugata 7 Askja, University of Iceland, IS 101 Reykjavik,  
6 Iceland. [jo@hi.is](mailto:jo@hi.is)

7 <sup>2</sup> Marine and Freshwater Research Institute, Fornubúðir 5, IS 220 Hafnafjörður, Iceland

8 <sup>3</sup> Lamont-Doherty Earth Observatory of Columbia University, Palisades, NY 10964, U.S.A.

9 <sup>4</sup> National Energy Authority, Grensásvegur 9, IS 108 Reykjavík, Iceland

10 <sup>5</sup> Deceased

11  
12 **Abstract**

13 The North Atlantic north of 50°N is one of the most intense ocean sink areas for atmospheric  
14 CO<sub>2</sub> considering the flux per unit area, 0.27 Pg-C yr<sup>-1</sup>, equivalent to -2.5 mol C m<sup>-2</sup> yr<sup>-1</sup>. The  
15 Northwest Atlantic Ocean is a region with high anthropogenic carbon inventories. This is on  
16 account of processes which sustain CO<sub>2</sub> air-sea fluxes, in particular strong seasonal winds,  
17 ocean heat loss, deep convective mixing and CO<sub>2</sub> drawdown by primary production. The  
18 region is in the northern limb of the Global Thermohaline Circulation, a path for the long term  
19 deep sea sequestration of carbon dioxide. The surface water masses in the North Atlantic are  
20 of contrasting origins and character, on the one hand the northward flowing North Atlantic  
21 Drift, a Gulf Stream offspring, on the other hand southward moving cold low salinity Polar  
22 and Arctic Waters with signatures from Arctic freshwater sources. We have studied by  
23 observations, the CO<sub>2</sub> air-sea flux of the relevant water masses in the vicinity of Iceland in all  
24 seasons and in different years. Here we show that the highest ocean CO<sub>2</sub> influx is to the  
25 Arctic and Polar waters, respectively, -3.8 mol C m<sup>-2</sup> yr<sup>-1</sup> and -4.4 mol C m<sup>-2</sup> yr<sup>-1</sup>. These  
26 waters are CO<sub>2</sub> undersaturated in all seasons. The Atlantic Water is a weak or neutral sink,  
27 near CO<sub>2</sub> saturation, after poleward drift from subtropical latitudes. These characteristics of  
28 the three water masses are confirmed by data from observations covering 30 years. We relate  
29 the Polar and Arctic Water persistent undersaturation and CO<sub>2</sub> influx to the excess alkalinity  
30 derived from Arctic sources, ~~particularly the Arctic rivers.~~ Carbonate chemistry equilibrium  
31 calculations indicate clearly that the excess alkalinity may support a significant portion of the  
32 North Atlantic CO<sub>2</sub> sink. The Arctic contribution to the North Atlantic CO<sub>2</sub> sink which we  
33 reveal is previously unrecognized. However, we point out that there are gaps and conflicts in  
34 the knowledge about the Arctic alkalinity budget and carbonate budgets and that future trends  
35 in the North Atlantic CO<sub>2</sub> sink are connected to developments in the rapidly warming and

Formatted: Numbering: Continuous

Formatted: Font color: Auto

Formatted: Font color: Auto

Formatted: Font color: Auto

Formatted: Font: Bold, No underline

36 ~~changing~~ Arctic. The results we present need to be taken into consideration for the question:  
37 Will the North Atlantic continue to absorb CO<sub>2</sub> in the future as it has in the past?

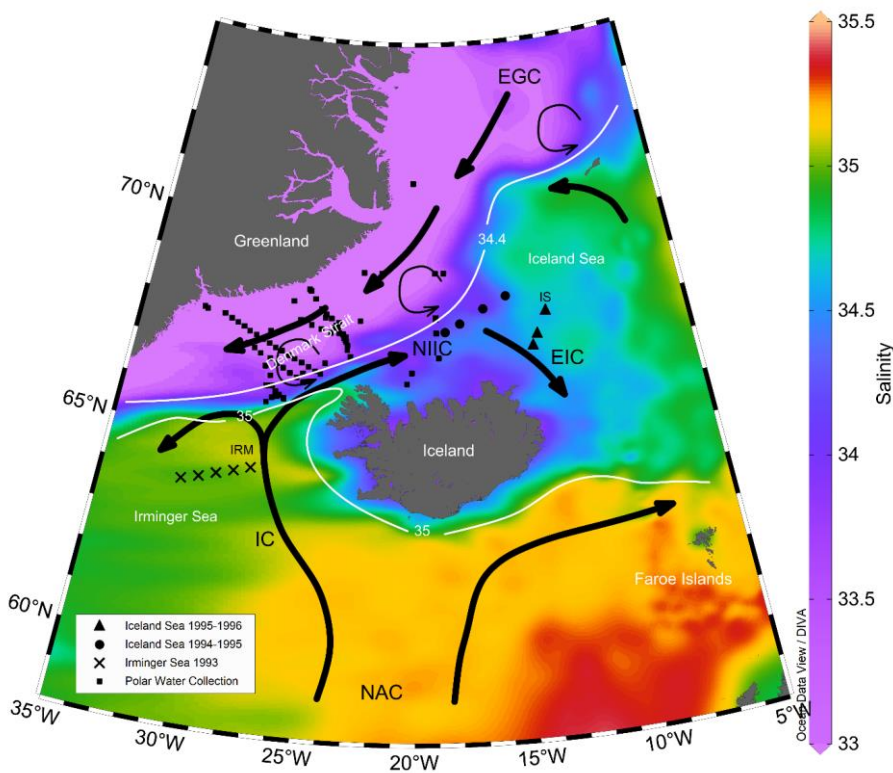
## 39 1 Introduction

40 The oceans take up about a quarter of the annual anthropogenic CO<sub>2</sub> emissions (Friedlingstein  
41 et al., 2019)–. ~~This may even be an underestimate (Watson et al., 2020)~~. The North Atlantic  
42 north of 50°N is one of the most intense ocean sink areas for atmospheric CO<sub>2</sub> considering the  
43 flux per unit area (Takahashi et al., 2009). The reasons are strong winds and large natural  
44 partial pressure differences,  $\Delta p\text{CO}_2 = (p\text{CO}_{2\text{sw}} - p\text{CO}_{2\text{a}})$ , between the atmosphere and the  
45 surface ocean. The  $\Delta p\text{CO}_2$  in seawater is a measure of the escaping tendency of CO<sub>2</sub> from  
46 seawater to the overlying air. The  $\Delta p\text{CO}_2$  is proportional to the concentration of  
47 undissociated CO<sub>2</sub> molecules, [CO<sub>2</sub>]aq, which constitutes about 1 % of the total CO<sub>2</sub>  
48 dissolved in seawater (the remainders being about 90-95 % as [HCO<sub>3</sub><sup>-</sup>] and 4-9 % as [CO<sub>3</sub><sup>2-</sup>]).  
49 The seawater  $p\text{CO}_2$  depends sensitively on temperature and the TCO<sub>2</sub>/Alk ratio, the relative  
50 concentrations of total CO<sub>2</sub> species dissolved in seawater (TCO<sub>2</sub> = [CO<sub>2</sub>]aq + [HCO<sub>3</sub><sup>-</sup>] +  
51 [CO<sub>3</sub><sup>2-</sup>]) and the alkalinity, Alk, which reflects the ionic balance in seawater. Large  $\Delta p\text{CO}_2$   
52 has been attributed to, a) a cooling effect on the CO<sub>2</sub> solubility in the poleward flowing  
53 Atlantic Water, b) an efficient biological drawdown of  $p\text{CO}_2$  in nutrient rich subpolar waters  
54 and c) high wind speeds over these low  $p\text{CO}_2$  waters (Takahashi et al., 2002). Evaluations of  
55  $\Delta p\text{CO}_2$  based on observation and models have indicated that the Atlantic north of 50°N and  
56 northward into the Arctic takes up as much as 0.27 Pg-C yr<sup>-1</sup>, equivalent to -2.5 mol C m<sup>-2</sup> yr<sup>-1</sup>  
57 (Takahashi et al., 2009; Schuster et al., 2013; Landschützer et al., 2013; Mikaloff Fletcher et al.,  
58 2006). ~~Estimates~~The North Atlantic is a relatively well observed region of the ocean (Lauvset  
59 et al., 2016). ~~Nevertheless, estimates~~ of long term trends for the North Atlantic CO<sub>2</sub> sink due  
60 to changes in either  $\Delta p\text{CO}_2$  or wind strength are conflicting, particularly the Atlantic Water  
61 dominated regions (Schuster et al., 2013; Landschützer et al., 2013; Wanninkhof et al., 2013).  
62 The drivers of seasonal flux variations are considered inadequately understood (Schuster et  
63 al., 2013) and a mechanistic understanding of high latitude CO<sub>2</sub> sinks is ~~considered~~regarded  
64 incomplete (McKinley et al., 2017). It ~~is~~has been common to many large scale flux  
65 evaluations, modelled or from observations, that they are based on regions defined by  
66 geographical borders, latitude and longitude, e.g. between 49°N and 76°N for the high latitude  
67 Sub Polar North Atlantic (Takahashi et al., 2009; Schuster et al., 2013). ~~The influence of~~  
68 ~~oceanographic property differences within this region on CO<sub>2</sub> fluxes has thus not been~~

Formatted: Font: Bold, No underline

Formatted: No underline

69 apparent, primarily due to Arctic latitude data limitations. A more realistic approach is to  
 70 define biogeographical regions, biomes (Fay and McKinley, 2014). The influence of  
 71 oceanographic property differences within this region on CO<sub>2</sub> fluxes has generally not been  
 72 apparent, primarily due to Arctic latitude data limitations. The ability of current generation  
 73 Earth System Models to predict trends in North Atlantic CO<sub>2</sub> has recently been questioned  
 74 and suggested that their inadequacies may be caused by biased alkalinity in the simulated  
 75 background biogeochemical state (Lebehot et al., 2019).



76  
 77 **Figure 1. Mean July to September surface salinity in the vicinity of Iceland.** The  $S=35$   
 78 isohaline marks the boundary between northward flowing Atlantic Water and southward  
 79 flowing cold Arctic Water and low salinity Polar Water. Stations in Irminger Sea marked X  
 80 and stations in Iceland Sea marked ● for 1994-1995 and ▲ for 1995-1996 observations.  
 81 Collection of Polar Water stations 1983-2012 marked ■. IRM and IS mark the location of time  
 82 series stations. NAC: North Atlantic Current, IC: Irminger Current, NIIC: North Iceland  
 83 Irminger Current, EIC: East Icelandic Current, EGC: East Greenland Current. Map based

84 on the NISE dataset (Nilsen et al., 2008) and drawn using the Ocean Data View program  
85 (Schlitzer, 2018).

86  
87

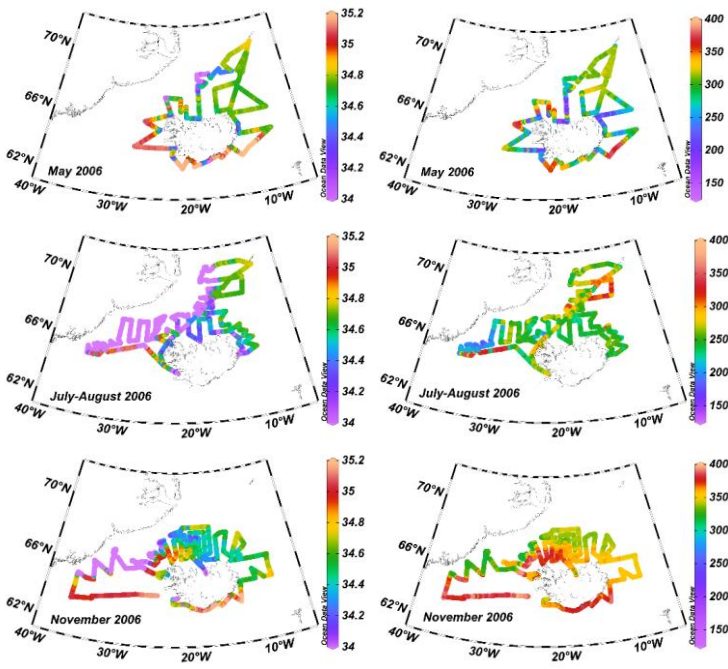
88 Here we evaluate regional, seasonal and interannual air-sea carbon dioxide fluxes for the main  
89 surface waters characteristic of this region (Fig. 1). We base this work on extensive  
90 observations which cover regional water masses, all seasons and include different states of the  
91 North Atlantic Oscillation, NAO (Flatau et al., 2003). We employ two different observation  
92 approaches for flux estimates. Firstly, repeat station hydrography with emphasis on the  
93 seasonal flux patterns in Atlantic Water and in Arctic Water (Fig. 1). Secondly, underway  
94 ship records of surface  $p\text{CO}_2$  where the emphasis was on the different surface water masses  
95 (Fig. 2).

96

97

98

99



100

101

102

103

104

105

106

107

108

109

110

111

112

113

114

115

116

117

118

119

120

121

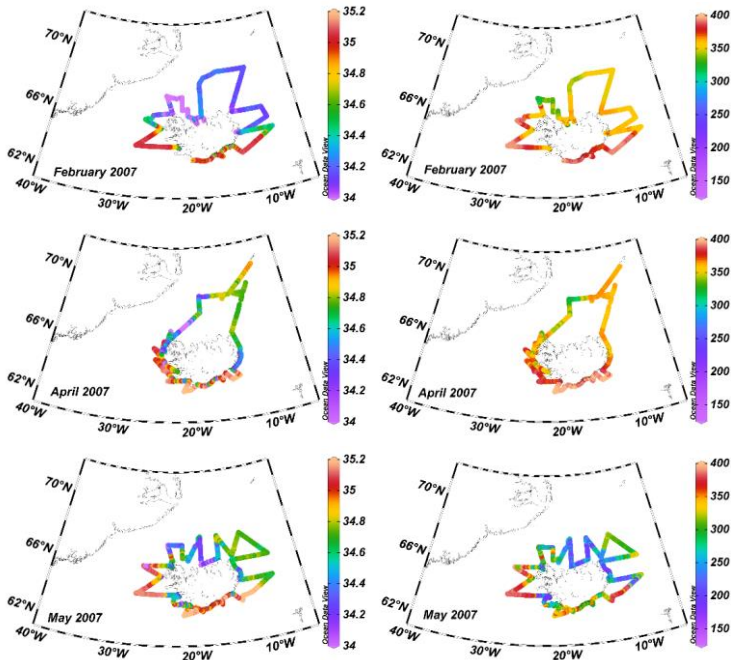


**Figure 2. Cruise tracks where surface layer salinity and  $p\text{CO}_2$  were recorded underway.** Left sea surface salinity, right  $p\text{CO}_2\text{sw}(\mu\text{atm})$  along the cruise tracks. Maps drawn using the Ocean Data View program (Schlitzer, 2018).

We describe long term carbon chemistry characteristics of water masses in mid winter when physical forces prevail over biological processes. For the Irminger Sea and Iceland Sea from time series observations (Olafsson et al., 2010) and for the EGC Polar Water from a collection of  $p\text{CO}_2$  data assembled in the period 1983 to 2012.

## 2 Methods

### 2.1 Data acquisition

#### 2.1.1 Seasonal studies 1993-1996

Seasonal carbon chemistry variations in the relatively warm and saline ( $S > 35$ ) Atlantic Water were studied 1993-1994 on 15 cruises from February 1993 to January 1994 to 5 stations on a 167 km long transect over the core of the Irminger Current and into the northern Irminger Sea (Fig. 1 and Tables S1 and S2). In order to close the full annual cycle, to 23 February 1994 we

122 use data from the previous year and date. In 1994-1996 the study centered on the colder and  
123 less saline Arctic Water of the Iceland Sea and was conducted on 22 cruises with sampling  
124 dates from 11 Feb 1994 to 12 Feb 1996, two years. In 1994 on 4 stations on a 168 km long  
125 transect into the Iceland Sea Gyre and in 1995 on 3 stations across the East Icelandic Current  
126 (Fig. 1 and Tables S1 and S3 in the supplement). On each cruise the station work was  
127 completed in 1-2 days. For both regions, the timing of cruises was with the period of the  
128 phytoplankton spring bloom in mind (~~Takahashi et al., 1993b~~)(Takahashi et al., 1993). The  
129 work was conducted on vessels operated by the Marine Research Institute (MRI) in  
130 Reykjavik, Iceland, R/V Bjarni Seamundsson and R/V Arni Fridriksson. Three times in 1994  
131 a fishing vessel M/V Solrun, was hired. In August 1994 the stations were completed on the  
132 Norwegian vessel R/V Johann Hjort.

133 Discrete surface layer, 1m, 5m and 10m,  $p\text{CO}_2$  samples were collected into 500 ml volumetric  
134 flasks and total dissolved inorganic carbon samples,  $\text{TCO}_2$ , into 250 ml flasks from water  
135 bottles on a Rosette and Sea Bird 911 CTD instruments. The  $p\text{CO}_2$  samples were preserved  
136 with mercuric chloride and analysed ashore by equilibration at 4°C with a gas of known  $\text{CO}_2$   
137 concentration followed by gas chromatography with a flame ionization detector. The  
138 instrument was calibrated with  $\text{N}_2$  reference gas and 3 standards, 197.85 ppm, 362.6 ppm and  
139 811.08 ppm, calibrated against standards certified by NOAA-CMDL at Boulder, CO, USA.  
140 So were also calibrated the standards used for the underway measurements (Chipman et al.,  
141 1993). Samples for total dissolved inorganic carbon,  $\text{TCO}_2$ , were similarly preserved with  
142 mercuric chloride and analysed by coulometry ashore. Quality assurance and sample storage  
143 experiments indicated an overall precision of the discrete sample  $p\text{CO}_2$  determinations better  
144 than  $\pm 2 \mu\text{atm}$  and of the  $\text{TCO}_2$  determinations  $\pm 2 \mu\text{mol kg}^{-1}$  after 1990 but  $\pm 4 \mu\text{mol kg}^{-1}$   
145 earlier (Olafsson et al., 2010).

146

### 147 2.1.2 Underway $p\text{CO}_2$ records 2006-2007

148 The underway  $p\text{CO}_2$  determinations in 2006-2007 covered areas of the East Greenland  
149 Current in and northwards from the Denmark Strait, in addition to Atlantic and Arctic Waters.  
150 The 6 cruises (Table S4) covered all seasons and all three water masses but with variable areal  
151 extensions (Fig. 2-~~and S4~~). Seawater was pumped continuously from an intake at 5 m depth  
152 at  $10 \text{ L min}^{-1}$  into a shower-head equilibrator with a total volume of 30 L and a headspace of  
153 15 L. Temperature at the inlet and salinity were measured with an SeaBird Model SBE-21  
154 thermosalinograph (Sea-Bird Electronics, Seattle, WA, USA). Underway  $p\text{CO}_2$  determinations  
155 were carried out with a system similar to the one described by Bates and coworkers (Bates et

156 al., 1998). The mole fraction of CO<sub>2</sub> (V CO<sub>2</sub>) in the headspace was determined with a Li-Cor  
157 infrared analyzer Model 6251 (Li-Cor Biosciences, Lincoln, NB, USA). The instrument was  
158 calibrated against four standards of CO<sub>2</sub> in air certified by NOAA-CMDL at Boulder, CO,  
159 USA. and a N<sub>2</sub> reference gas. The standards had CO<sub>2</sub> dry air mole fractions of 122.19,  
160 253.76, 358.41 and 476.81 ppm. The pCO<sub>2</sub> sw determinations were corrected to in-situ  
161 seawater temperatures using the equation (Takahashi et al., ~~1993~~1993):

162  $p\text{CO}_2 \text{ sw(in situ)} = p\text{CO}_2 \text{ sw(eq)} e^{0.0423(T_{\text{in situ}} - T_{\text{eq}})}$  (eq.1)

163 ~~The sample processing and quality control measures have been described in detail (Ólafsson~~  
164 ~~et al., 2010).~~

165

### 166 **2.1.3 Time series data**

167 We use discrete sample pCO<sub>2</sub>, TCO<sub>2</sub> and calculated Total Alkalinity data from the Irminger  
168 Sea and the Iceland Sea time series stations (Ólafsson, 2012, 2016).

169

### 170 **2.1.4 Polar Water data collection-**

171 Discrete samples for carbon chemistry studies were taken on stations (N=~~97146~~) in the East  
172 Greenland Current when opportunities permitted on cruises in the period 1983 to 2012. The 25  
173 m surface layer data provide include >400 TCO<sub>2</sub> samples and >300 pairs of pCO<sub>2</sub> and TCO<sub>2</sub>  
174 for calculation of ~~Delta pCO<sub>2</sub> in Fig. 4~~ carbonate system parameters. The seasonal cycle by  
175 month is evaluated from the composite data.

176

### 177 **2.1.5 Carbonate chemistry calculations**

178 The most desirable way for computing carbonate chemistry parameters is to use pCO<sub>2</sub> and  
179 TCO<sub>2</sub> (Takahashi et al., 2014). We calculate Total alkalinity from discrete sample pCO<sub>2</sub> and  
180 TCO<sub>2</sub> data pairs using the CO2SYS.xls v2.1 software (Lewis and Wallace, 1998; Pierrot et al.,  
181 2006) and select carbonic acid dissociation constants (Lueker et al., 2000), the constant for  
182 HSO<sub>4</sub><sup>-</sup> (Dickson, 1990) and boron concentrations (Lee et al., 2010).

183

### 184 **2.2 CO<sub>2</sub> air-sea flux calculations**

185 In this study, the pCO<sub>2</sub> partial pressure of carbon dioxide in seawater samples has been  
186 measured by gas-seawater equilibration methods (Ólafsson et al., 2010). The results are  
187 expressed as pCO<sub>2</sub>. The bulk flux of the carbon dioxide across the air-sea interface is often  
188 estimated from its relationship with wind speed and sea-air partial pressure difference,

Field Code Changed

189  $\Delta p\text{CO}_2$ . We determine the flux (F) from  $\Delta p\text{CO}_2$  and use Eq. 42 and Eq. 23 for estimating the  
190 bulk air-sea fluxes of  $\text{CO}_2$  (Takahashi et al., 2009)

$$191 F = k \cdot \alpha \cdot \Delta p\text{CO}_2 \quad (\text{Eq 42})$$

$$192 F = 0.251 U^2 (Sc/660)^{-0.5} \alpha (p\text{CO}_{2w} - p\text{CO}_{2a}) \quad (\text{Eq 23})$$

193 There  $k=0.251 U^2 (Sc/660)^{-0.5}$  is the gas transfer velocity or kinetic component of the  
194 expression (Wanninkhof, 2014),  $\alpha$  is the solubility of  $\text{CO}_2$  gas in sea water (Weiss, 1974) and  
195  $\Delta p\text{CO}_2 = (p\text{CO}_{2sw} - p\text{CO}_{2a})$ , is the partial pressure difference or thermodynamic component of  
196 the expression (Takahashi et al., 2009). For the wind speed, U, we use the CCMP-2  
197 reanalysis wind product (Wanninkhof, 2014; Atlas et al., 2011; Wanninkhof and Triñanes,  
198 2017).

199 The atmospheric partial pressure values,  $p\text{CO}_{2a}$ , used in the  $\Delta p\text{CO}_2$  calculations are weekly  
200 averages from the GLOBALVIEW-CO2 database for the CO2-ICE location which is at  
201 Vestmannaeyjar islands, off south Iceland (GLOBALVIEW-CO2, 2013). Mauna Loa values  
202 were used for periods where CO2-ICE data was missing (Tans and Keeling, 2019). ~~The dry~~  
203 ~~air  $V \text{CO}_2$  mole fraction values were converted to  $\mu\text{atm}$  using  $p\text{CO}_2 (\mu\text{atm}) = V \text{CO}_2 (P_a - P_w)$~~   
204 ~~where  $P_a$  is the barometric pressure and  $P_w$  is the equilibrium water vapour pressure. The dry~~  
205 ~~air  $V \text{CO}_2$  mole fraction values were converted to  $\mu\text{atm}$  using  $p\text{CO}_2 (\mu\text{atm}) = V \text{CO}_2 (P_a - P_w)$~~   
206 ~~where  $P_a$  is the barometric pressure and  $P_w$  is the equilibrium water vapour pressure (Weiss~~  
207 ~~and Price, 1980).~~

209 For the underway cruises 2006 to 2007 we used CCMP-2 daily wind fields at 1x1 degree for  
210 the region 62°N to 72°N and 5°W to 40°W. This region was further divided into 4 sub-  
211 regions by latitude 64.9°N and longitude 20°W. Daily 30 day running means of the squared  
212 wind speed from two locations in each sub-region were extracted and their means used for  
213 flux calculations when the vessel sailed in the area. Fluxes were calculated for all  $p\text{CO}_2$  data  
214 from the 6 cruises, in total 42938 measurements.

215 The flux data from each of the 6 cruises were categorized into the three sea water types using  
216 the following criteria:

- 217 1) Atlantic Water  $S > 35$ , Arctic Water  $S: 34.4-34.9$ , Polar Water  $S < 34.4$ .
- 218 2) Seasonal salinity and temperature variations were taken into account.
- 219 3) Waters with runoff influences from Iceland were excluded using salinity and ship  
220 position data.

221 Thus a total of 33352 measurements were used, or 78% of the flux data points. The CO<sub>2</sub>  
222 fluxes in the realm of each water mass were assessed for the duration of each cruise by  
223 numerical integration. Fluxes in the 5 periods between cruises were assessed by interpolation  
224 of temperature, salinity and pCO<sub>2</sub> for each water mass and by using period regional 30 day  
225 running means of squared wind speed data. The annual flux for each water mass was assessed  
226 by summation.

227

### 228 **3 Results**

229 ~~Mean monthly reanalysis of winds reveal~~**3.1 Seasonal variations and annual CO<sub>2</sub> fluxes at**  
230 **regional water masses**

231 ~~The wind gas transfer coefficient reveals~~ seasonal variations ~~with~~**reflecting** strong winds in  
232 winter when they may be stronger over the Irminger Sea than the Iceland Sea as in 1993-1994

|

|

238

233 ~~and in 1994-1995 (Fig. 3).~~

---

  
234 studies reveal the strongest CO<sub>2</sub> undersaturation, with negative  $\Delta p\text{CO}_2$  of about 100  $\mu\text{atm}$  in  
235 May at the time of the phytoplankton spring bloom (Fig. 4 3b). The undersaturation diminishes  
236 through the summer and autumn followed by a gradual return to winter conditions (Fig. 4b) (Takahashi  
237 et al., 1985; Peng et al., 1987; Takahashi et al., 1993a, 1993).

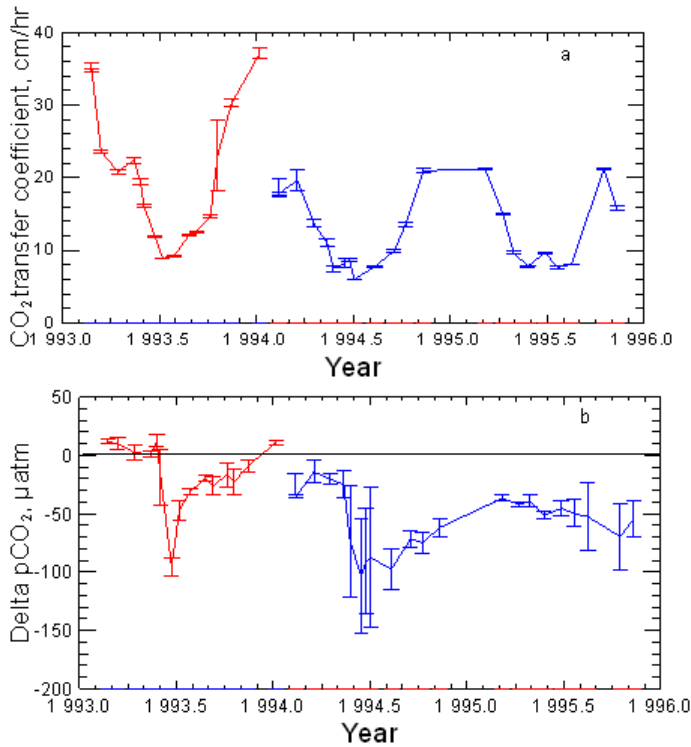


**Figure 43.** Seasonal variations in the Atlantic Water of the Irminger Sea (red) and in the Arctic Water of the Iceland Sea (blue). The gas transfer velocity (a) reflects the seasonal wind strength and the error bars its variations during intervals between cruises. Delta pCO<sub>2</sub> (b) records the tendency for CO<sub>2</sub> to be transferred to the atmosphere (positive) or from the atmosphere to the ocean (negative). The CO<sub>2</sub> flux rate (c) reveals that the Arctic Water is a CO<sub>2</sub> sink in all seasons whereas the Atlantic Water is a source in winter and a weak sink at other times of the year. The error bars indicate ± 1 standard deviation from the mean and reflect the variations between the stations observed each cruise.

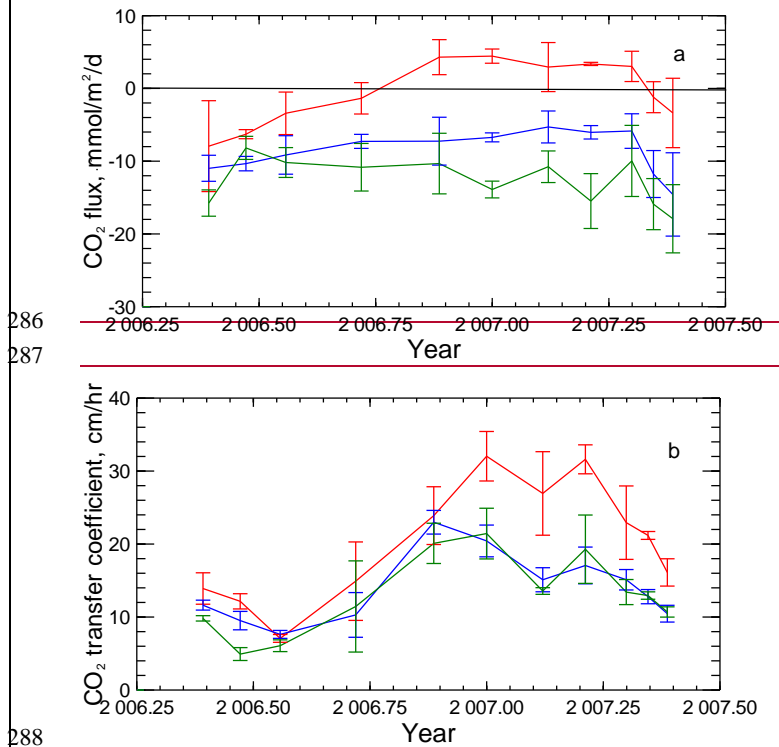
The CO<sub>2</sub> influx in the spring is, however, relatively small as the wind gas transfer coefficient is then moderate (Fig. 4a 3a). In the autumn the winds strengthen with heat loss and vertical mixing while CO<sub>2</sub> undersaturation still persists. In mid winter, February-March, vertical mixing brings richer CO<sub>2</sub> water to the surface of the Irminger Sea leading to supersaturation (Ólafsson, 2003), the flux reverses and the region becomes a weak source for atmospheric CO<sub>2</sub> (Fig. 4e3c).

**Table 1** Annual sea-air CO<sub>2</sub> fluxes (mol C m<sup>-2</sup> y<sup>-1</sup>) in the three water masses.

Water masses and evaluation methods	CO <sub>2</sub> flux mol C m <sup>-2</sup> y <sup>-1</sup>
Atlantic water, repeat stations 1993	-0.69±0.16
Atlantic water, Underway Measurements, 2006-2007	0.07 ± 0.15
Arctic water, repeat stations 1994	-3.97±0.48
Arctic water, repeat stations 1995	-3.60±0.31
Arctic water, Underway Measurements, 2006-2007	-2.84 ± 0.19
Polar water, Underway Measurements, 2006-2007	-4.44 ± 0.34

259  
260 The integrated annual CO<sub>2</sub> flux shows that the Atlantic Water in the Irminger Sea was a weak  
261 sink, -0.69±0.16 mol C m<sup>-2</sup> y<sup>-1</sup>, in 1993 (Table 1). The more extensive underway area  
262 coverage of the Atlantic Water in 2006-2007, confirmed in essence the seasonal pattern and  
263 indicated that the Atlantic Water was a neutral sink, 0.07 ± 0.15 mol C m<sup>-2</sup> y<sup>-1</sup> for this year  
264 (Table 1). The winter gas transfer coefficient was again significantly larger over the Atlantic  
265 Water regions than the Arctic and Polar Waters, facilitating air-sea equilibration (Fig. 4b).  
266 The years of the Iceland Sea observations, 1994-1996, coincided with a large transition in the  
267 North Atlantic Oscillation (NAO) from a positive state 1994/1995 to a negative state in  
268 1995/1996 and large scale shifts in ocean fronts (Flatau et al., 2003). Vertical density  
269 distribution in the Iceland Sea indicated an enhanced convective activity in 1995 (Våge et al.,  
270 2015). Cold northeasterly winds were persistent in the spring of 1995 resulting in record low  
271 temperature anomalies for the north Iceland shelf (Ólafsson, 1999). In 1995 the spring bloom  
272 associated undersaturation, ΔpCO<sub>2</sub>, was only half of that in 1994, possibly due to a weaker  
273 stratification (Fig. 4b). In 1995 the spring bloom associated undersaturation, ΔpCO<sub>2</sub>, was only  
274 half of that in 1994, possibly due to a weaker stratification in May and and continued over the  
275 summer season (Fig.S2) (Våge et al., 2015). As in the Irminger Sea the spring bloom  
276 associated CO<sub>2</sub> influx is small. The largest CO<sub>2</sub> influx was in the fall and early winters of  
277 1995 and 1996 as temperature dropped, winds gathered strength and vertical mixing was  
278 enhanced. This compensated for the small spring bloom in 1995 and the annual bulk  
279 fluxes 1994 and 1995 are similar and high despite very different physical conditions  
280 (Table 1). The UWpCO<sub>2</sub> surveys had less temporal resolution but confirmed all year  
281 undersaturation of the Arctic Water. However, the integrated annual influx, -2.84 mol C m<sup>-2</sup> y<sup>-1</sup>,  
282 was significantly less than evaluated with repeat station data (Table 1, Fig.5)-even though  
283 the strength of the gas transfer coefficient was similar in both studies (Table 1, Figs.4a and

284 **4b).** This may reflect the large underway area coverage compared with the repeated fixed  
285 stations.



288  
289 **Figure 54. Seasonal air-sea CO<sub>2</sub> flux variations from UWpCO<sub>2</sub> observations.**  
290 *a)* Atlantic Water (red) is a weak sink in summer and neutral over the year, n=7068. Both  
291 Arctic Water (blue) n=16874, and Polar Water (green) n=9410, are strong sinks throughout  
292 the year. The error bars indicate ± 1 standard deviation from the mean. *b)* The gas transfer  
293 coefficient for the Atlantic Water regime is significantly stronger in winter than for the Arctic  
294 and Polar Water.

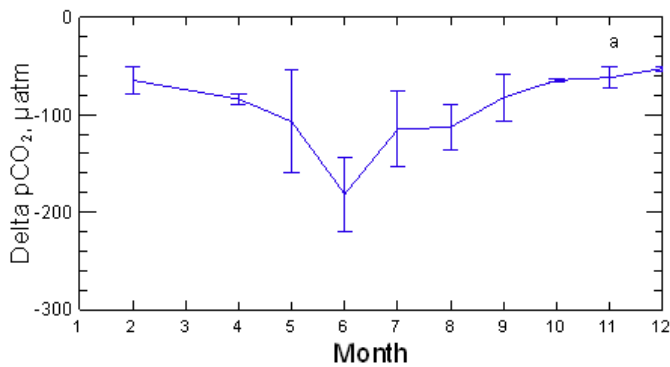
295  
296 Ice cover in the East Greenland Current is variable and the ice edge at the seasonal minimum  
297 has moved northward and from the Denmark Strait with decreasing Arctic sea ice (Serreze  
298 and Meier, 2019). The Polar Water salinity ranges from 34.4 to less than 30 in summer. The  
299 lowest salinity water freezes leading to salinity around 34 in winter. We covered the Polar  
300 Water in all six UWpCO<sub>2</sub> surveys 2006-2007 (Supplement-Fig. S42) and undersaturation  
301 characterised this water mass in all cruises. The integrated annual influx, -4.44 mol C m<sup>-2</sup> y<sup>-1</sup>  
302 (Table 1, Fig. 54), shows the Polar Water to be the strongest CO<sub>2</sub> sink, 80 % above the  
303 estimated mean for the Atlantic north of 50°N, -2.5 mol C m<sup>-2</sup> y<sup>-1</sup> (Takahashi et al., 2009).

304 Further comparison with the Takahashi climatology indicates a broad agreement with Arctic  
305 Water region NE of Iceland with -3.5 to -4.5 mol C m<sup>-2</sup> y<sup>-1</sup> and with the Atlantic Water region  
306 S and SW of Iceland with about -1 mol C m<sup>-2</sup> y<sup>-1</sup> (Takahashi et al., 2009).

### 308 **3.2 Long term $\Delta p\text{CO}_2$ characteristics of the regional water masses**

309 We evaluate the long term  $p\text{CO}_2$  characteristics of the three water ~~masses~~ masses from three  
310 other  
311 data assembled over about 30 years. ~~We use the Polar Water data collection and draft a~~  
312 composite picture of seasonal  $\Delta p\text{CO}_2$  variations in Polar Water in and north of the Denmark  
313 Strait (Fig. 1) confirms all year undersaturation, deep ~~from biological drawdown~~ in summer,  
314 and in mid winter when salinity raises to  $\sim 34$ , the  $\Delta p\text{CO}_2$  levels at about  $-50 \mu\text{atm}$  (Fig. ~~6a5a~~).  
315 Long term winter  $\Delta p\text{CO}_2$  in the Irminger Sea and Iceland Sea (Figs. 1 and ~~6~~ b5b) when  
316 biological activity is minimal (Olafsson et al., 2009), show the Atlantic Water to be near saturation, slightly  
317 supersaturated and following the atmospheric  $p\text{CO}_2$  increase of  $1.80 \mu\text{atm/yr.}$  whereas the  
318 Arctic Water is undersaturated to about  $-35 \mu\text{atm}$ . The Gulf Stream derived Atlantic Water  
319 which reaches the northern Irminger Sea and the Nordic Seas, has had a long contact time  
320 with the atmosphere to loose heat and reach near  $\text{CO}_2$  saturation (Takahashi et al., 2002; Olsen  
321 et al., 2006).

Field Code Changed



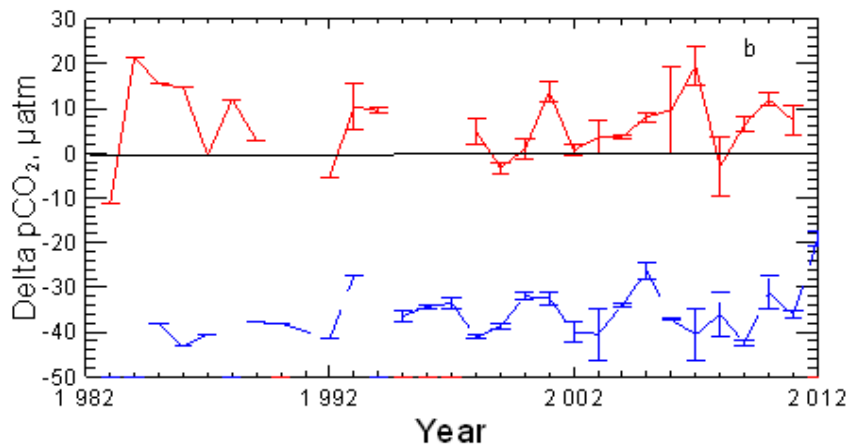


**Figure 65. Water mass decadal surface water pCO<sub>2</sub> characteristics.** a) A composite picture of Delta pCO<sub>2</sub> from 97146 stations with Polar Water pCO<sub>2</sub> observations (n=280)312) from the 25 m surface layer 1983 to 2012 shows undersaturation at all times of the year. The error bars indicate ± 1 standard deviation from the monthly means. b) Atlantic Water at the Irminger Sea time series station (red) is generally a weak CO<sub>2</sub> source in winter (24 winters, 52 samples), January-March, whereas winter (25 winters, 61 samples) CO<sub>2</sub> undersaturation persists ~~in~~at the Iceland Sea time series site (blue). The error bars indicate ± 1 standard deviation from the surface layer station means.

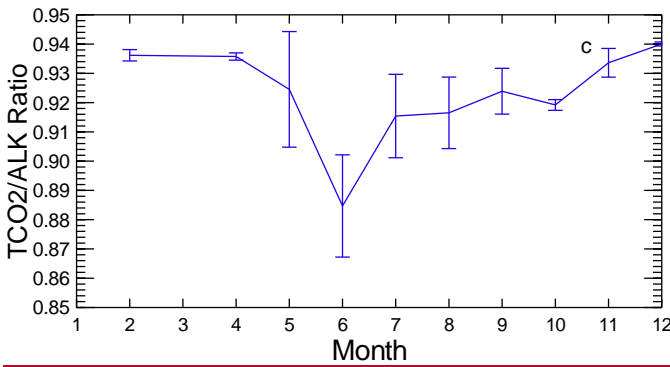
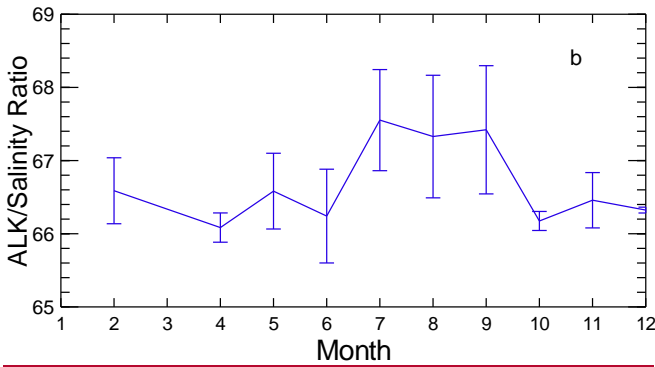
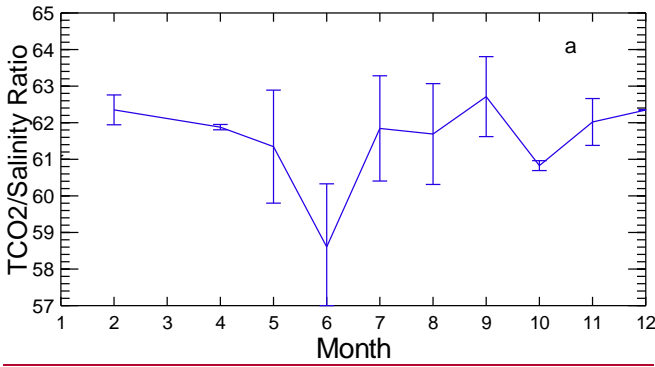
The Polar Water in the East Greenland Current which is advected southward from the Arctic is in general characterised by low temperature and large seasonal salinity and carbonate chemistry variations. Both physical and biogeochemical processes generate the large seasonal variability but the winter observations represent the state of lowest biological activity (Fig. 6) (Table 2). The TCO<sub>2</sub> data in Table 2 are uncorrected for hydrographic variations or anthropogenic trends but the Atlantic Water is based on a short period of 10 years and the Polar Water atmospheric contact history is poorly known.

**Table 2. Mean IRM-TS Atlantic Water surface layer conditions in winter, 2001-2010 and in Polar Water 25 m surface layer November to April 1984-2012.**

	T °C	Salinity, S	Density, ρ kg/m <sup>3</sup>	TCO <sub>2</sub> /S	ALK/S	TCO <sub>2</sub> /ALK	pCO <sub>2</sub> µatm
Atlantic Water	7.11 ± 0.36	35.13 ± 0.03	1027.507 ± 0.034	61.11 ± 0.09	65.96 ± 0.13	0.926 ± 0.002	388 ± 9

<u>Polar</u>	<u>-0.31</u>	<u>33.95</u>	<u>1027.255</u>	<u>62.16</u>	<u>66.49</u>	<u>0.935</u>	<u>301</u>
<u>Water</u>	<u>±1.53</u>	<u>± 0.33</u>	<u>± 0.244</u>	<u>±0.54</u>	<u>± 0.40</u>	<u>± 0.004</u>	<u>±11</u>

343  
 344 The winter conditions in the northward flowing Atlantic Water at the Irminger Sea time series  
 345 station 2001-2010 (Table 2) are in stark contrast and with notably higher  $p\text{CO}_2$  and lower  
 346  $\text{TCO}_2/\text{S}$  and  $\text{ALK}/\text{S}$  ratios than the Polar Water in winter.



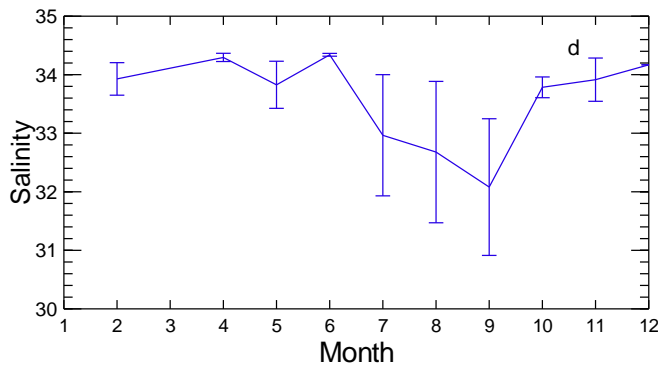


**Figure 6. Polar Water seasonal carbonate chemistry variations.** Composite Polar Water data from the 25m surface layer. The seasonal variations in the a) Total inorganic carbon/Salinity ratio, b) Alkalinity/Salinity ratio and c) Total inorganic carbon/Alkalinity ratio reflect biological carbon assimilation and inorganic processes associated with fresh water inputs which lower the salinity d) to the annual minimum in late summer. The red horizontal lines mark the Atlantic Water benchmarks (Table 2).

We take the Atlantic Water in winter (Table 2) as a proxy (benchmark) for the relatively warm and saline water advected from the North Atlantic to the Nordic Seas and the Arctic and compare with it the carbonate chemistry seasonal variations in the southward flowing Polar Water (Fig. 6). The ALK/S ratio for the Polar Water is higher than that for the Atlantic Water in winter and throughout the year (Fig. 6b). The TCO<sub>2</sub>/S ratio of the Polar Water is larger than that of the Atlantic Water except in early summer when biological assimilation, photosynthesis, decreases the TCO<sub>2</sub> concentration. The TCO<sub>2</sub>/ALK ratio falls as a consequence (Fig. 6c) which leads to strong pCO<sub>2</sub> undersaturation and large Delta pCO<sub>2</sub> (Figs 6e and 5a). The high TCO<sub>2</sub>/S and ALK/S ratios indicate alkalinity and carbonate inputs as freshwater lowers the Polar Water salinity to a minimum in late summer (Fig. 6d).

#### 4 Discussion

The Polar Water TCO<sub>2</sub>/S and ALK/S ratios (Table 2 and Fig. 6) indicate both alkalinity and dissolved carbonate additions. The choice of winter ratios (Table 2) as benchmarks is solely for the evaluation of seasonal changes in the Polar Water. Representative annual long term TCO<sub>2</sub>/S and ALK/S means would be more realistic but are not available. Still, such a TCO<sub>2</sub>/S ratio would expectedly be lower than the winter one. An assessment of the effects of the

375 relative TCO<sub>2</sub> and ALK additions to Polar Water depends on the benchmarks chosen (Table  
376 1).

377 The carbonate chemistry of Polar Water differs from that of open ocean waters, e.g. Atlantic  
378 Water, in having an increasingly higher alkalinity/salinity and alkalinity/TCO<sub>2</sub> ratios as the  
379 salinity decreases from about S=34.4. The excess alkalinity has been attributed to the high  
380 riverine input from continents to the Arctic (~~Anderson et al., 2004; Lee et al., 2006~~)(Anderson  
381 et al., 2004). The flow-weighted average alkalinity of 6 major Arctic rivers, discharging 2.245  
382 x 10<sup>3</sup> km<sup>3</sup> yr<sup>-1</sup>, is 1048 μmol kg<sup>-1</sup>, however, without assessed uncertainty (Cooper et al.,  
383 2008). The river runoff into the Arctic is estimated to be about 4.2 x 10<sup>3</sup> km<sup>3</sup> yr<sup>-1</sup>, or 0.133 x  
384 10<sup>6</sup> m<sup>3</sup> s<sup>-1</sup> (0.133 Sv). This is about 11% of the global freshwater input to the oceans  
385 (Carmack et al., 2016). Taking the average alkalinity 1048 μmol kg<sup>-1</sup>, the amount of  
386 alkalinity added by rivers to the Arctic and transported to the North Atlantic via the Canadian  
387 Arctic Arcipelago and via the Fram Strait and further south with the Labrador and East  
388 Greenland Currents, would be 4.4 x 10<sup>12</sup> mol yr<sup>-1</sup> (Supplement). ~~Cooper et al. (2008) reported~~  
389 on riverine alkalinity but not on associated inorganic carbonate. A recent assessment of Polar  
390 Water boron concentrations indicates insignificant borate contribution with Arctic rivers  
391 (Olafsson et al., 2020). The riverine alkalinity may primarily be attributed to carbonate  
392 alkalinity, CA=[HCO<sub>3</sub><sup>-</sup>]+2[CO<sub>3</sub><sup>2-</sup>]. The potential of the added alkalinity to reduce pCO<sub>2</sub> of  
393 seawater would depend on its excess over TCO<sub>2</sub>.

394 Linear alkalinity-salinity relationships observed in the Arctic Ocean and the Nordic Seas and  
395 their extrapolated intercepts to S=0, have indicated freshwater sources with alkalinity 1412  
396 μmol kg<sup>-1</sup> (Anderson et al., 2004) and 1752 μmol kg<sup>-1</sup> (Nondal et al., 2009). Climatological  
397 data from the West- Greenland, Iceland and Norwegian Seas show a high S=0 intercept of  
398 1796 μmol kg<sup>-1</sup> but a lower one for the High Arctic north of 80°N, ~~1341 μmol~~ 1341 μmol kg<sup>-1</sup>  
399 (Takahashi et al., 2014)~~-. The climatological relationships were for Potential Alkalinity,~~  
400 PA=TA + NO<sub>3</sub><sup>-</sup>, which has little influence since the nitrate concentrations are low. The  
401 intercepts may be interpreted as the mean alkalinity of fresh waters added to the Arctic by  
402 rivers and melting ice and snow. However, the above intercepts indicate considerable  
403 variability, they are also higher than the average alkalinity of Arctic rivers ~~and the intercepts~~  
404 are high in upstream regions of the East Greenland Current, 1048 μmol kg<sup>-1</sup>. The excess  
405 alkalinity would lower the pCO<sub>2</sub> in seawater (and increase the pH), and thus give it an  
406 increased capacity to take up CO<sub>2</sub> from the air (Fig. 7). The thermodynamic driving force for  
407 seawater CO<sub>2</sub> uptake, (pCO<sub>2sw</sub> - pCO<sub>2a</sub>), ~~is~~ would be enhanced.

409 The difference between the average measured Arctic river alkalinity and the regression based  
410 estimates of alkalinity sources suggests that other origins and processes than the rivers  
411 contribute to the Polar Water alkalinity exported with currents from the Arctic to the Atlantic  
412 Ocean. Photic layer primary production in the absence of calcification may lower ~~the~~  
413 ~~TCO<sub>2</sub>hTCO<sub>2</sub>~~/Alk ratio and seawater  $p\text{CO}_2$  in marginal seas (Bates, 2006), while  
414 acidification is increasing in other regions (Anderson et al., 2017; Qi et al., 2017)- and  
415 projected to become extensive at the end of the century (Terhaar et al., 2020). Furthermore,  
416 the sea-ice seasonal formation and melting may affect the TCO<sub>2</sub>/Alk ratio (Grimm et al.,  
417 2016; Rysgaard et al., 2007). Efforts to reconstruct alkalinity fields and alkalinity climatology  
418 for the Arctic have however been difficult (Broullón et al., 2019).

420 The Arctic is complex and complex climate warming related changes are observed in the  
421 western Arctic Ocean (Ouyang et al., 2020) and expected in marine freshwater systems of the  
422 warming Arctic (Carmack et al., 2016). Not least is the ice cover and areas of multi-year ice  
423 decreasing (Serreze and Meier, 2019). River water alkalinity increases with an addition of  
424 cations derived from the chemical weathering of silicate and carbonate rocks (Berner and  
425 Berner, 1987). Accordingly, an increase in Arctic weathering rates, in response to warmer  
426 climate and increasing atmospheric CO<sub>2</sub>, could increase the river water alkalinity transported  
427 into the oceans. Such an increase would lower the  $p\text{CO}_2$  in seawater and enhance the oceanic  
428 uptake of atmospheric CO<sub>2</sub>, providing a negative feedback mechanism to the climatic  
429 warming resulting from increased atmospheric CO<sub>2</sub>.

## 431 5 Conclusions

432 ~~The North Atlantic region we describe has ocean waters advected from southern temperate~~  
433 ~~latitudes and others from the north with Arctic signatures.~~The North Atlantic region we  
434 describe has Atlantic Waters advected from southern temperate latitudes and cold lower  
435 salinity Arctic and Polar Waters carried with the East Greenland Current from the Arctic. The  
436 Atlantic Water seasonal  $p\text{CO}_2$  variations are primarily driven by regional thermal and  
437 biological cycles but without much net annual influx of CO<sub>2</sub>.~~The Gulf Stream derived~~  
438 ~~Atlantic Water which reaches the northern Irminger Sea and the Nordic Seas, has had a long~~  
439 ~~and the Atlantic Water (AW) sinks in the North Atlantic Ocean (NAO) and the Arctic Ocean (AO) and~~  
440 ~~the Atlantic Water (AW) sinks in the North Atlantic Ocean (NAO) and the Arctic Ocean (AO) and~~  
441 year CO<sub>2</sub> sinks despite various regional changes upstream in the Arctic Ocean. Downstream  
442 from the Polar Water and Arctic Water outflows. These waters are advected towards the sub-  
polar North Atlantic with high inventories of anthropogenic carbon. The TCO<sub>2</sub>/S and ALK/S

443 Polar Water ratios are higher than those for the Atlantic Water indicating carbonate and  
444 alkalinity sources. is the subpolar North Atlantic with high water column inventories of  
445 atmospheric CO<sub>2</sub> and alkalinity. The high CO<sub>2</sub> and alkalinity inventories are likely to be  
446 additional unrecognized source contributing to the North Atlantic CO<sub>2</sub> sink. -Climate induced  
447 changesWe also see that there are gaps and conflicts in the knowledge about the Arctic  
448 biogeochemistry and alkalinity budget are likely to affect the sensitivity and carbonate  
449 budgets and that future strength of trends in the North Atlantic CO<sub>2</sub> sink downstream are  
450 connected to developments in the rapidly warming and changing Arctic.

#### 452 Acknowledgements

453 The NMR Nordic Environmental Research Programme: Carbon Cycle and Convection in the  
454 Nordic Seas, supported the Marine Research Institute (MRI), Reykjavik, repeat station study  
455 in 1993-1995. The MRI work in 2006-2008 was supported by the European Union 6th  
456 Framework Program CARBOOCEAN, EU Contract: 511176. Taro Takahashi was supported  
457 to work on the manuscript with a grant from the the US National Oceanographic and  
458 Atmospheric Administration. The CCMP-2 wind product was generously provided ~~by~~from  
459 Remote Sensing Systems ([www.remss.com/measurements/CCMP](http://www.remss.com/measurements/CCMP)) by Dr. Joaquin Triñanes  
460 of CIMAS/AOML, Miami. We gratefully acknowledge the long term technical support from  
461 John Goddard and Tim Newberger, Lamont-Doherty Earth Observatory. We are grateful for  
462 the invaluable cooperation we have had with the crews of all vessels operated in this study  
463 and to Norwegian colleagues for providing time for station work in August 1994.

466 *Author Contributions.* J.O., T.T. and S.R.O. wrote the manuscript. J.O., Th.S.A., S.R.O. and  
467 M.D. conducted the fieldwork. J.O., T.T. S.R.O. and Th.S.A., conceived this study.

#### 469 Additional information

471 The underway pCO<sub>2</sub> data is available at Ocean Carbon Data System (OCADS) (Takahashi et  
472 al., 2019). The Irminger Sea and Iceland Sea seasonal study data and the Polar Water  
473 collection data are stored at the Marine and Freshwater Research Institute, Reykjavik and  
474 available by request. Irminger Sea and Iceland Sea time series data for calculation of Delta

Field Code Changed

Formatted: Font color: Auto

Formatted: Font color: Auto

476 [pCO<sub>2</sub> in winter is at NOAA National Centers for Environmental Information \(Ólafsson, 2016,](#)  
477 [2012\).](#)

## 478 **References**

- 480  
481 ~~Anderson, L. G., Jutterström, S., Kaltin, S., and Jones, E. P.: Variability in river runoff~~  
482 ~~distribution in the Eurasian Basin of the Arctic Ocean, *Journal of Geophysical Research*, 109,~~  
483 ~~doi:10.1029/2003JC001733, 2004.~~
- 484 Anderson, L. G., Ek, J., Ericson, Y., Humborg, C., Semiletov, I., Sundbom, M., and Ulfso,  
485 A.: Export of calcium carbonate corrosive waters from the East Siberian Sea, *Biogeosciences*,  
486 14, 1811-1823, 10.5194/bg-14-1811-2017, 2017.
- 487 Atlas, R., Hoffman, R. N., Ardizzone, J., Leidner, S. M., Jusem, J. C., Smith, D. K., and  
488 Gombos, D.: A cross-calibrated multiplatform ocean surface wind velocity product for  
489 meteorological and oceanographic applications, *Bull. Amer. Meteor. Soc.*, 92, 157-174,  
490 10.1109/IGARSS.2008.4778804, 2011.
- 491 Bakker, D. C. E., Pfeil, B., Landa, C. S., Metzl, N., O'Brien, K. M., Olsen, A., Smith, K.,  
492 Cosca, C., Harasawa, S., Jones, S. D., Nakaoka, S., Nojiri, Y., Schuster, U., Steinhoff, T.,  
493 Sweeney, C., Takahashi, T., Tilbrook, B., Wada, C., Wanninkhof, R., Alin, S. R., Balestrini,  
494 C. F., Barbero, L., Bates, N. R., Bianchi, A. A., Bonou, F., Boutin, J., Bozec, Y., Burger, E.  
495 F., Cai, W. J., Castle, R. D., Chen, L., Chierici, M., Currie, K., Evans, W., Featherstone, C.,  
496 Feely, R. A., Fransson, A., Goyet, C., Greenwood, N., Gregor, L., Hankin, S., Hardman-  
497 Mountford, N. J., Harlay, J., Hauck, J., Hoppema, M., Humphreys, M. P., Hunt, C. W., Huss,  
498 B., Ibáñez, J. S. P., Johannessen, T., Keeling, R., Kitidis, V., Körtzinger, A., Kozyr, A.,  
499 Krasakopoulou, E., Kuwata, A., Landschützer, P., Lauvset, S. K., Lefèvre, N., Lo Monaco,  
500 C., Manke, A., Mathis, J. T., Merlivat, L., Millero, F. J., Monteiro, P. M. S., Munro, D. R.,  
501 Murata, A., Newberger, T., Omar, A. M., Ono, T., Paterson, K., Pearce, D., Pierrot, D.,  
502 Robbins, L. L., Saito, S., Salisbury, J., Schlitzer, R., Schneider, B., Schweitzer, R., Sieger, R.,  
503 Skjelvan, I., Sullivan, K. F., Sutherland, S. C., Sutton, A. J., Tadokoro, K., Telszewski, M.,  
504 Tuma, M., van Heuven, S. M. A. C., Vandemark, D., Ward, B., Watson, A. J., and Xu, S.: A  
505 multi-decade record of high-quality fCO<sub>2</sub> data in version 3 of the Surface Ocean CO<sub>2</sub> Atlas  
506 (SOCAT), *Earth Syst. Data*, 8, 383-413, 10.5194/essd-8-383-2016, 2016.
- 507 Bates, N. R., Takahashi, T., Chipman, D. W., and Knap, A. H.: Variability of pCO<sub>2</sub> on diel to  
508 seasonal timescales in the Sargasso Sea near Bermuda, *Journal of Geophysical Research:*  
509 *Oceans*, 103, 15567-15585, 10.1029/98jc00247, 1998.
- 510 Bates, N. R.: Air-sea CO<sub>2</sub> fluxes and the continental shelf pump of carbon in the Chukchi Sea  
511 adjacent to the Arctic Ocean, *Journal of Geophysical Research: Oceans*, 111,  
512 10.1029/2005jc003083, 2006.
- 513 Berner, E. K., and Berner, R. A.: *The Global Water Cycle, Geochemistry and Environment*,  
514 Prentice-Hall, Englewood Cliffs, NJ, 1987.
- 515 Broecker, W. S.: The Great Ocean Conveyor, *Oceanography*, 4, 79-89, 1991.
- 516 Broullón, D., Pérez, F. F., Velo, A., Hoppema, M., Olsen, A., Takahashi, T., Key, R. M.,  
517 Tanhua, T., González-Dávila, M., Jeansson, E., Kozyr, A., and van Heuven, S. M. A. C.: A  
518 global monthly climatology of total alkalinity: a neural network approach, *Earth Syst. Sci.*  
519 *Data*, 11, 1109-1127, 10.5194/essd-11-1109-2019, 2019.
- 520 Carmack, E. C., Yamamoto-Kawai, M., Haine, T. W. N., Bacon, S., Bluhm, B. A., Lique, C.,  
521 Melling, H., Polyakov, I. V., Straneo, F., Timmermans, M.-L., and Williams, W. J.:  
522 Freshwater and its role in the Arctic Marine System: Sources, disposition, storage, export, and  
523 physical and biogeochemical consequences in the Arctic and global oceans, *J. Geophys. Res.*  
524 *Biogeosci.*, 121, 675-717, doi:10.1002/2015JG003140, 2016.

525 Chipman, D., Marra, J., and Takahashi, T.: Primary production at 47°N and 20°W in the  
526 North Atlantic Ocean: a comparison between the <sup>14</sup>C incubation method and the mixed layer  
527 budget, *Deep Sea Research II*, 40, 151-169, 1993.

528 Cooper, L. W., McClelland, J. W., Holmes, R. M., Raymond, P. A., Gibson, J. J., C. K. Guay,  
529 and Peterson, B. J.: Flow-weighted values of runoff tracers ( $\delta^{18}\text{O}$ , DOC, Ba, alkalinity) from  
530 the six largest Arctic rivers, *Geophysical Research Letters*, 35, doi:10.1029/2008GL035007,  
531 2008.

532 Dickson, A. G.: Standard Potential of the Reaction - AgCl(S)+1/2H<sub>2</sub>(G)=Ag(S)+HC l(Aq)  
533 and the Standard Acidity Constant of the ion HSO<sub>4</sub><sup>-</sup> in Synthetic Sea-Water from 273.15-K to  
534 318.15-K, *J Chem Thermodyn*, 22, 113-127, Doi 10.1016/0021-9614(90)90074-Z, 1990.

535 Dickson, R. P., Meincke, J., Malmberg, S. A., and Lee, A. J.: The Great salinity Anomaly in  
536 the northern North Atlantic, *Progress in Oceanography*, 20, 103-151, 1988.

537 Fay, A. R., and McKinley, G. A.: Global open-ocean biomes: mean and temporal variability,  
538 *Earth Syst. Sci. Data*, 6, 273-284, 10.5194/essd-6-273-2014, 2014.

539 Flatau, M. K., Talley, L., and Niiler, P. P.: The North Atlantic Oscillation, surface current  
540 velocities, and SST changes in the subpolar North Atlantic, *Journal of Climate*, 16, 2355-  
541 2369, 2003.

542 Friedlingstein, P., Jones, M. W., O'Sullivan, M., Andrew, R. M., Hauck, J., Peters, G. P.,  
543 Peters, W., Pongratz, J., Sitch, S., Le Quééré, C., Bakker, D. C. E., Canadell, J. G., Ciais, P.,  
544 Jackson, R. B., Anthoni, P., Barbero, L., Bastos, A., Bastrikov, V., Becker, M., Bopp, L.,  
545 Buitenhuis, E., Chandra, N., Chevallier, F., Chini, L. P., Currie, K. I., Feely, R. A., Gehlen,  
546 M., Gilfillan, D., Gkritzalis, T., Goll, D. S., Gruber, N., Gutekunst, S., Harris, I., Haverd, V.,  
547 Houghton, R. A., Hurtt, G., Ilyina, T., Jain, A. K., Joetzjer, E., Kaplan, J. O., Kato, E., Klein  
548 Goldewijk, K., Korsbakken, J. I., Landschützer, P., Lauvset, S. K., Lefèvre, N., Lenton, A.,  
549 Lienert, S., Lombardozzi, D., Marland, G., McGuire, P. C., Melton, J. R., Metzl, N., Munro,  
550 D. R., Nabel, J. E. M. S., Nakaoka, S. I., Neill, C., Omar, A. M., Ono, T., Peregon, A., Pierrot,  
551 D., Poulter, B., Rehder, G., Resplandy, L., Robertson, E., Rödenbeck, C., Séférian, R.,  
552 Schwinger, J., Smith, N., Tans, P. P., Tian, H., Tilbrook, B., Tubiello, F. N., van der Werf, G.  
553 R., Wiltshire, A. J., and Zaehle, S.: Global Carbon Budget 2019, *Earth Syst. Sci. Data*, 11,  
554 1783-1838, 10.5194/essd-11-1783-2019, 2019.

555 GLOBALVIEW-CO<sub>2</sub>: Cooperative Global Atmospheric Data Integration Project. 2013,  
556 updated annually. Multi-laboratory compilation of synchronized and gap-filled atmospheric  
557 carbon dioxide records for the period 1979-2012 obspack\_co2\_1\_GLOBALVIEW-  
558 CO<sub>2</sub>\_2013\_v1.0.4\_2013-12-23, 2013.

559 Grimm, R., Notz, D., Glud, R. N., Rysgaard, S., and Six, K. D.: Assessment of the sea-ice  
560 carbon pump: Insights from a three-dimensional ocean-sea-ice-biogeochemical model  
561 (MPIOM/HAMOCC), *Elementa: Science of the Anthropocene*, 4, doi:  
562 10.12952/journal.elementa.000136  
563 elementascience.org, 2016.

564 Gruber, N., Clement, D., Carter, B. R., Feely, R. A., van Heuven, S., Hoppema, M., Ishii, M.,  
565 Key, R. M., Kozyr, A., Lauvset, S. K., Lo Monaco, C., Mathis, J. T., Murata, A., Olsen, A.,  
566 Perez, F. F., Sabine, C. L., Tanhua, T., and Wanninkhof, R.: The oceanic sink for  
567 anthropogenic CO<sub>2</sub> from 1994 to 2007, *Science*, 363, 1193-1199, 10.1126/science.aau5153,  
568 2019.

569 Haine, T. W. N., Curry, B., Gerdes, R., Hansen, E., Karcher, M., Lee, C., Rudels, B., Spreen,  
570 G., Steur, L. d., Stewart, K. D., and Woodgate, R.: Arctic freshwater export: Status,  
571 mechanisms, and prospects, *Global and Planetary Change*, 125, 13-35, 2015.

572 Håvik, L., Pickart, R. S., Våge, K., Torres, D., Thurnherr, A. M., Beszczynska-Möller, A.,  
573 Walczowski, W., and Appen, W.-J. v.: Evolution of the East Greenland Current from Fram

574 Strait to Denmark Strait: Synoptic measurements from summer 2012, *J. Geophys. Res.*  
575 *Oceans*, 122, 1974-1994, doi:10.1002/2016JC01222, 2017.

576 Hátún, H., Sandø, A. B., Drange, H., Hansen, B., and Valdimarsson, H.: Influence of the  
577 Atlantic Subpolar Gyre on the Thermohaline Circulation, *Science*, 309, 1841-1844, 2005.

578 Holliday, N. P., Bersch, M., Berx, B., Chafik, L., Cunningham, S., Florindo-López, C., Hátún,  
579 H., Johns, W., Josey, S. A., Larsen, K. M. H., Mulet, S., Oltmanns, M., Reverdin, G., Rossby,  
580 T., Thierry, V., Valdimarsson, H., and Yashayaev, I.: Ocean circulation causes the largest  
581 freshening event for 120 years in eastern subpolar North Atlantic, *Nature Communications*,  
582 11, 585, 10.1038/s41467-020-14474-y, 2020.

583 Khatiwala, S., Tanhua, T., Mikaloff Fletcher, S., Gerber, M., Doney, S. C., Graven, H. D.,  
584 Gruber, N., McKinley, G. A., Murata, A., Ríos, A. F., and Sabine, C. L.: Global ocean storage  
585 of anthropogenic carbon, *Biogeosciences*, 10, 2169-2191, 10.5194/bg-10-2169-2013, 2013.

586 Landschützer, P., Gruber, N., Bakker, D. C. E., Schuster, U., Nakaoka, S., Payne, M. R.,  
587 Sasse, T. P., and Zeng, J.: A neural network-based estimate of the seasonal to inter-annual  
588 variability of the Atlantic Ocean carbon sink, *Biogeosciences*, 10, 7793-7815, 10.5194/bg-10-  
589 7793-2013, 2013.

590 Lauvset, S. K., Key, R. M., Olsen, A., van Heuven, S., Velo, A., Lin, X., Schirnack, C.,  
591 Kozyr, A., Tanhua, T., Hoppema, M., Jutterström, S., Steinfeldt, R., Jeansson, E., Ishii, M.,  
592 Perez, F. F., Suzuki, T., and Watelet, S.: A new global interior ocean mapped climatology: the  
593  $1^\circ \times 1^\circ$  GLODAP version 2, *Earth Syst. Sci. Data*, 8, 325-340, 10.5194/essd-8-325-2016,  
594 2016.

595 Lebehot, A. D., Halloran, P. R., Watson, A. J., McNeall, D., Ford, D. A., Landschützer, P.,  
596 Lauvset, S. K., and Schuster, U.: Reconciling Observation and Model Trends in North  
597 Atlantic Surface CO<sub>2</sub>, *Global Biogeochemical Cycles*, 33, 1204-1222,  
598 10.1029/2019gb006186, 2019.

599 Lee, K., Kim, T.-W., Byrne, R. H., Millero, F. J., Feely, R. A., and Liu, Y.-M.: The universal  
600 ratio of boron to chlorinity for the North Pacific and North Atlantic oceans, *Geochimica et*  
601 *Cosmochimica Acta*, 74, 1801-1811, 2010.

602 Lewis, E., and Wallace, D.: Programme developed for CO<sub>2</sub> system calculations, Carbon  
603 Dioxide Information Analysis Center, Oak Ridge National Laboratory, U.S. Department of  
604 Energy/ORN/CDIAC-105, 1998.

605 Lueker, T. J., Dickson, A. G., and Keeling, C. D.: Ocean pCO<sub>2</sub> calculated from dissolved  
606 inorganic carbon, alkalinity, and equations for K-1 and K-2: validation based on laboratory  
607 measurements of CO<sub>2</sub> in gas and seawater at equilibrium, *Marine Chemistry*, 70, 105-119,  
608 Doi 10.1016/S0304-4203(00)00022-0, 2000.

609 McClelland, J. W., Holmes, R. M., Dunton, K. H., and Macdonald, R. W.: The Arctic Ocean  
610 Estuary, *Estuaries and Coasts*, 35, 353-368, DOI 10.1007/s12237-010-9357-3, 2012.

611 McKinley, G. A., Fay, A. R., Lovenduski, N. S., and Pilcher, D. J.: Natural Variability and  
612 Anthropogenic Trends in the Ocean Carbon Sink, *Annu. Rev. Mar. Sci.*, 9, 125-150,  
613 10.1146/annurev-marine-010816-060529, 2017.

614 Mikaloff Fletcher, S. E., Gruber, N., Jacobson, A. R., Doney, S. C., Dutkiewicz, S., Gerber,  
615 M., Follows, M., Joos, F., Lindsay, K., Menemenlis, D., Mouchet, A., Iler, S. A. M.,  
616 Sarmiento, J. L., et al. (2006), and *Global Biogeochem. Cycles*, GB2002,  
617 doi:10.1029/2005GB002530.: Inverse estimates of anthropogenic CO<sub>2</sub> uptake, transport, and  
618 storage by the ocean, *Global Biogeochem. Cycles*, 20, doi:10.1029/2005GB002530, 2006.

619 Nilsen, J. E. Ø., Hátún, H., Mork, K. A., and Valdimarsson, H.: The NISE Dataset, *Faroese*  
620 *Fisheries Laboratory*, Box 3051, Tórshavn, Faroe Islands, 2008.

621 Nondal, G., Bellerby, R., Olsen, A., Johannessen, T., and Olafsson, J.: Predicting the surface  
622 ocean CO<sub>2</sub> system in the northern North Atlantic: Implications for the use of Voluntary  
623 Observing Ships., *Limnology and Oceanography: Methods*, 7, 109-118, 2009.

624 Olafsson, J., Olafsdottir, S. R., Benoit-Cattin, A., Danielsen, M., Arnarson, T. S., and  
625 Takahashi, T.: Rate of Iceland Sea acidification from time series measurements,  
626 *Biogeosciences*, 6, 2661-2668, 2009.

627 Olafsson, J., Olafsdottir, S. R., Benoit-Cattin, A., and Takahashi, T.: The Irminger Sea and the  
628 Iceland Sea time series measurements of sea water carbon and nutrient chemistry 1983–2008,  
629 *Earth Syst. Sci. Data*, 2, 99-104, 10.5194/essd-2-99-2010, 2010.

630 Olafsson, J., Lee, K., Olafsdottir, S. R., Benoit-Cattin, A., Lee, C.-H., and Kim, M.: Boron to  
631 salinity ratios for Atlantic, Arctic and Polar Waters: A view from downstream, *Marine*  
632 *Chemistry*, 224, 103809, <https://doi.org/10.1016/j.marchem.2020.103809>, 2020.

633 Olsen, A., Omar, A. M., Bellerby, R. G. J., Johannessen, T., Ninnemann, U., Brown, K. R.,  
634 Olsson, K. A., Olafsson, J., Nondal, G., Kivimae, C., Kringstad, S., Neill, C., and Olafsdottir,  
635 S.: Magnitude and Origin of the Anthropogenic CO<sub>2</sub> Increase and <sup>13</sup>C Suess Effect in the  
636 Nordic Seas Since 1981, *Global Biogeochemical Cycles*, 20, GB3027,  
637 doi:10.1029/2005GB002669, 2006.

638 Ouyang, Z., Qi, D., Chen, L., Takahashi, T., Zhong, W., DeGrandpre, M. D., Chen, B., Gao,  
639 Z., Nishino, S., Murata, A., Sun, H., Robbins, L. L., Jin, M., and Cai, W.-J.: Sea-ice loss  
640 amplifies summertime decadal CO<sub>2</sub> increase in the western Arctic Ocean, *Nature Climate*  
641 *Change*, 10, 678-684, 10.1038/s41558-020-0784-2, 2020.

642 Ólafsson, J.: Connections between oceanic conditions off N-Iceland, Lake Mývatn  
643 temperature, regional wind direction variability and the North Atlantic Oscillation, *Rit*  
644 *Fiskideildar*, 16, 41-57, 1999.

645 Ólafsson, J.: Winter mixed layer nutrients in the Irminger and Iceland Seas, 1990-2000, *ICES*  
646 *Marine Science Symposia*, 219, 329-332, 2003.

647 Ólafsson, J.: Partial pressure (or fugacity) of carbon dioxide, dissolved inorganic carbon,  
648 temperature, salinity and other variables collected from discrete samples, profile and time  
649 series profile observations during the R/Vs Arni Fridriksson and Bjarni Saemundsson time  
650 series IcelandSea (LN6) cruises in the North Atlantic Ocean from 1985-02-22 to 2013-11-26  
651 (NCEI Accession 0100063). Information, N. N. C. f. E. (Ed.), NOAA National Centers for  
652 Environmental Information, 2012.

653 Ólafsson, J.: Partial pressure (or fugacity) of carbon dioxide, dissolved inorganic carbon,  
654 temperature, salinity and other variables collected from discrete sample and profile  
655 observations using CTD, bottle and other instruments from ARNI FRIDRIKSSON and  
656 BJARNI SAEMUNDSSON in the North Atlantic Ocean from 1983-03-05 to 2013-11-13  
657 (NCEI Accession 0149098). Information, N. N. C. f. E. (Ed.), 2016.

658 Peng, T.-H., Takahashi, T., Broecker, W. S., and Ólafsson, J.: Seasonal variability of carbon  
659 dioxide, nutrients and oxygen in the northern North Atlantic surface water, *Tellus*, 39B, 439-  
660 458, 1987.

661 Pierrot, D., Lewis, E., and Wallace, D. W. R.: MS Excel Program Developed for CO<sub>2</sub> System  
662 Calculations. ORNL/CDIAC-105a. Carbon Dioxide Information Analysis Center,  
663 doi: 10.3334/CDIAC/otg.CO2SYS\_XLS\_CDIAC105a. Oak Ridge National Laboratory, U.S.  
664 Department of Energy, Oak Ridge, Tennessee., Oak Ridge, Tennessee, 2006.

665 Qi, D., Chen, L., Chen, B., Gao, Z., Zhong, W., Feely, R. A., Anderson, L. G., Sun, H., Chen,  
666 J., Chen, M., Zhan, L., Zhang, Y., and Cai, W.-J.: Increase in acidifying water in the western  
667 Arctic Ocean, *Nature Clim. Change*, 7, 195-199, 10.1038/nclimate3228  
668 [http://www.nature.com/nclimate/journal/v7/n3/abs/nclimate3228.html#supplementary-](http://www.nature.com/nclimate/journal/v7/n3/abs/nclimate3228.html#supplementary-information)  
669 [information](http://www.nature.com/nclimate/journal/v7/n3/abs/nclimate3228.html#supplementary-information), 2017.

670 Rysgaard, S., Glud, R. N., Sej, M. K., Bendtsen, J., and Christensen, P. B.: Inorganic carbon  
671 transport during sea ice growth and decay: A carbon pump in polar seas, *Journal of*  
672 *Geophysical Research*, 112, 2007.

673 Schlitzer, R.: Ocean Data View, <http://odv.awi.de>, 2018.

674 Schuster, U., McKinley, G. A., Bates, N., Chevallier, F., Doney, S. C., Fay, A. R., González-  
675 Dávila, M., Gruber, N., Jones, S., Krijnen, J., Landschützer, P., Lefèvre, N., Manizza, M.,  
676 Mathis, J., Metzl, N., Olsen, A., Rios, A. F., Rödenbeck, C., Santana-Casiano, J. M.,  
677 Takahashi, T., Wanninkhof, R., and Watson, A. J.: An assessment of the Atlantic and Arctic  
678 sea-air CO<sub>2</sub> fluxes, 1990–2009, *Biogeosciences*, 10, 607-627, 10.5194/bg-10-607-2013,  
679 2013.

680 Serreze, M. C., and Meier, W. N.: The Arctic's sea ice cover: trends, variability, predictability,  
681 and comparisons to the Antarctic, *Annals of the New York Academy of Sciences*, 1436, 36-  
682 53, 10.1111/nyas.13856, 2019.

683 Stefánsson, U.: North Icelandic Waters, *Rit Fiskideildar*, 3, 1-269, 1962.

684 Sutherland, D. A., Pickart, R. S., Peter Jones, E., Azetsu-Scott, K., Jane Eert, A., and  
685 Ólafsson, J.: Freshwater composition of the waters off southeast Greenland and their link to  
686 the Arctic Ocean, *Journal of Geophysical Research: Oceans*, 114, 10.1029/2008jc004808,  
687 2009.

688 Takahashi, T., Ólafsson, J., Broecker, W. S., Goddard, J., Chipman, D. W., and White, J.:  
689 Seasonal variability of the carbon-nutrient chemistry in the ocean areas west and north of  
690 Iceland, *Rit Fiskideildar*, 9, 20-36, 1985.

691 Takahashi, T., Ólafsson, J., Goddard, J. G., Chipman, D. W., and Sutherland, S. C.: Seasonal  
692 variation of CO<sub>2</sub> and nutrient salts over the high latitude oceans: A comparative study, *Global  
693 Biogeochemical Cycles*, 7, 843-878, 1993.

694 Takahashi, T., Sutherland, S. C., Sweeney, C., Poisson, A., Metzl, N., Tilbrook, T., Bates, N.,  
695 Wanninkhof, R., Feely, R. A., Sabine, C., Olafsson, J., and Nojiri, Y.: Global sea-air CO<sub>2</sub> flux  
696 based on climatological surface ocean pCO<sub>2</sub>, and seasonal biological and temperature effects,  
697 *Deep-Sea Research II*, 49, 1601-1622, 2002.

698 Takahashi, T., Sutherland, S. C., Wanninkhof, R., Sweeney, C., Feely, R. A., Chipman, D.  
699 W., Hales, B., Friederich, G., Chavez, F., Sabine, C., Watson, A., Bakker, D. C. E., Schuster,  
700 U., Metzl, N., Yoshikawa-Inoue, H., Ishii, M., Midorikawa, T., Nojiri, Y., Körtzinger, A.,  
701 Steinhoff, T., Hoppema, M., Olafsson, J., Arnarson, T. S., Tilbrook, B., Johannessen, T.,  
702 Olsen, A., Bellerby, R., Wong, C. S., Delille, B., Bates, N. R., and Baar, H. J. W. d.:  
703 Climatological mean and decadal change in surface ocean pCO<sub>2</sub>, and net sea-air CO<sub>2</sub> flux  
704 over the global oceans, *Deep-Sea Research II*, 56, 554-577, doi:10.1016/j.dsr2.2008.12.009,  
705 2009.

706 Takahashi, T., Sutherland, S. C., Chipman, D. W., Goddard, J. G., Ho, C., Newberger, T.,  
707 Sweeney, C., and Munro, D. R.: Climatological distributions of pH, pCO<sub>2</sub>, total CO<sub>2</sub>,  
708 alkalinity, and CaCO<sub>3</sub> saturation in the global surface ocean, and temporal changes at selected  
709 locations, *Marine Chemistry*, 164, 95-125, <http://dx.doi.org/10.1016/j.marchem.2014.06.004>,  
710 2014.

711 Takahashi, T., Sutherland, S. C., and Kozyr, A.: Global Ocean Surface Water Partial Pressure  
712 of CO<sub>2</sub> Database: Measurements Performed During 1957-2018 (LDEO Database Version  
713 2018) (NCEI Accession 0160492). Version 7.7. NOAA National Centers for Environmental  
714 Information. National Centers for Environmental Information, 2019.

715 Tans, P., and Keeling, R.: Mauna Loa CO<sub>2</sub> monthly mean data. NOAA/ESRL (Ed.), 2019.

716 Terhaar, J., Kwiatkowski, L., and Bopp, L.: Emergent constraint on Arctic Ocean  
717 acidification in the twenty-first century, *Nature*, 582, 379-383, 10.1038/s41586-020-2360-3,  
718 2020.

719 Våge, K., Pickart, R. S., Sarafanov, A., Knutsen, Ø., Mercier, H., Lherminier, P., van Aken,  
720 H. M., Meincke, J., Quadfasel, D., and Bacon, S.: The Irminger Gyre: Circulation,  
721 convection, and interannual variability, *Deep Sea Research Part I: Oceanographic Research  
722 Papers*, 58, 590-614, <https://doi.org/10.1016/j.dsr.2011.03.001>, 2011.

723 Våge, K., Pickart, R. S., Spall, M. A., Moore, G. W. K., Valdimarsson, H., Torres, D. J.,  
724 Y.Erofeeva, S., and Ø.Nilsen, J. E.: Revised circulation scheme north of the Denmark Strait,  
725 Deep-Sea Research Part I, 79, 20–39, 2013.

726 Våge, K., Moore, G. W. K., Jónsson, S., and Valdimarsson, H.: Water mass transformation in  
727 the Iceland Sea, Deep Sea Research Part I: Oceanographic Research Papers, 101, 98-109,  
728 <http://dx.doi.org/10.1016/j.dsr.2015.04.001>, 2015.

729 Wanninkhof, R., Park, G. H., Takahashi, T., Sweeney, C., Feely, R., Nojiri, Y., Gruber, N.,  
730 Doney, S. C., McKinley, G. A., Lenton, A., Le Quéré, C., Heinze, C., Schwinger, J., Graven,  
731 H., and Khatiwala, S.: Global ocean carbon uptake: magnitude, variability and trends,  
732 Biogeosciences, 10, 1983-2000, 10.5194/bg-10-1983-2013, 2013.

733 Wanninkhof, R.: Relationship between wind speed and gas exchange over the ocean revisited,  
734 Limnol. Oceanogr.: Methods, 12, 351–362, DOI 10.4319/lom.2014.12.351, 2014.

735 Wanninkhof, R., and Triñanes, J.: The impact of changing wind speeds on gas transfer and its  
736 effect on global air-sea CO<sub>2</sub> fluxes, Global Biogeochem. Cycles, 31,  
737 doi:10.1002/2016GB005592, 2017.

738 Watson, A. J., Schuster, U., Shutler, J. D., Holding, T., Ashton, I. G. C., Landschützer, P.,  
739 Woolf, D. K., and Goddijn-Murphy, L.: Revised estimates of ocean-atmosphere CO<sub>2</sub> flux are  
740 consistent with ocean carbon inventory, Nature Communications, 11, 4422, 10.1038/s41467-  
741 020-18203-3, 2020.

742 Weiss, R. F.: Carbon dioxide in water and seawater: The solubility of a non-ideal gas, Marine  
743 Chemistry, 2, 203-215, 1974.

744 Weiss, R. F., and Price, B. A.: Nitrous oxide solubility in water and seawater, Marine  
745 Chemistry, 8, 347-359, [https://doi.org/10.1016/0304-4203\(80\)90024-9](https://doi.org/10.1016/0304-4203(80)90024-9), 1980.

746